We sincerely thank the referee for the positive assessment of the scientific relevance and strengths of our study and for the constructive suggestions. We have carefully considered all the comments and have revised the terminology used for the observation periods, clarified the representativeness and uncertainty of the measurements, strengthened the event-classification procedure, added a sensitivity analysis for the estimated CCN concentrations, softened the interpretation of possible NPF mechanisms, and expanded the discussion of local urban emissions. Our point-by-point responses are provided below.

Comment 1:

The study is based on two relatively short observational campaigns: 9 October–10 November 2024 and 25 March–22 April 2025. While these measurements provide valuable insight into NPF characteristics during the selected monsoon and pre-monsoon periods, the limited duration may not fully represent the broader seasonal variability. The authors should add a short discussion on the representativeness of these campaign periods and clarify whether the reported seasonal differences can be generalized to typical monsoon and pre-monsoon conditions over Lhasa.

Response 1：

We thank the referee for this important comment. We agree that the two approximately one-month campaigns cannot fully represent the broader seasonal variability of NPF in Lhasa. Moreover, the October – November and March – April measurements do not correspond strictly to the summer monsoon and pre-monsoon seasons. We have therefore replaced "monsoon" and "pre-monsoon" with "autumn observation period" and "spring observation period," respectively, throughout the manuscript.

We have also revised the Abstract, Results and Discussion, and Conclusions to avoid generalizing the observed differences as representative seasonal patterns or mechanisms. The comparison is now explicitly described as a comparison between two campaign-based observation periods. We further acknowledge that interannual variability and the relatively short duration of each campaign may have influenced the observed NPF frequencies and atmospheric conditions. Longer-term continuous measurements covering complete annual cycles will be required to determine whether these differences are representative of typical autumn and spring conditions in Lhasa.

Comment 2:

The NPF event classification relies mainly on visual inspection of particle size distribution evolution. The authors should briefly clarify how classification uncertainty was handled, especially for weak or discontinuous events.

Response 2：

We thank the referee for this helpful suggestion. We have revised the event-classification method to reduce reliance on visual inspection alone. The original Class I and Class II categories were combined into a single "NPF day" category because their separation was not sufficiently robust. The revised classification consists of NPF, Undefined, and Non-Event days.

NPF days were identified primarily by the appearance of a distinct new particle mode at small diameters followed by identifiable growth toward larger sizes. Continuous growth throughout the entire day was not required because temporary interruptions may result from changes in air masses, boundary-layer development, variations in precursor availability, or missing measurements. For weak, discontinuous, or ambiguous cases, the PNSD interpretation was further supported by mean particle number concentrations in the 3–25 and 25–100 nm size ranges and candidate particle growth rates. These supporting parameters were used to improve classification transparency rather than as fixed thresholds.

Days showing enhanced small-particle concentrations or partial modal development but lacking sufficiently clear formation and subsequent growth were retained as Undefined days. To make the classification traceable, Table S1 now provides the revised day-by-day classification, NPF start and end times, size-segregated particle number concentrations, candidate GR calculation windows, and corresponding GR values. The daily PNSDs for NPF, Undefined, and Non-Event days are presented separately in Figs. S1–S3.

Comment 3:

Since CCN concentrations were estimated rather than directly measured, the authors should mention the uncertainty associated with the assumed κ value and supersaturation.

Response 3：

We thank the referee for pointing this out. We agree that the absolute estimated CCN concentrations depend on the assumed particle hygroscopicity and supersaturation. We have now explicitly stated throughout the manuscript that CCN concentrations were estimated from the measured PNSD using the κ-Köhler framework rather than directly measured.

We also conducted a sensitivity analysis using κ values of 0.08, 0.12, and 0.20 and supersaturations of 0.6 %, 0.8 %, and 1.2 % (Fig. S7). As expected, the assumed parameters substantially affected the critical activation diameter and the absolute estimated CCN concentrations. However, estimated CCN concentrations remained consistently higher during the autumn observation period than during the spring observation period across the tested parameter combinations. We have therefore clarified that the estimated CCN values are more suitable for interpreting relative differences and response patterns than for over-interpreting their absolute magnitudes.

Comment 4:

The possible role of VOCs in pre-monsoon particle growth is discussed, but VOCs were not measured. This point should be stated more cautiously.

Response 4：

We agree with the referee and have softened this interpretation. The revised manuscript no longer attributes spring particle growth to VOC-related oxidation. Instead, it states that a contribution from VOC-related oxidation cannot be excluded but cannot be constrained using the available measurements. We also explicitly acknowledge that VOCs, HOMs/OOMs, and their oxidation products were not directly measured, preventing quantitative attribution of their roles in particle formation or growth. The discussion and Conclusions have been revised accordingly.

Comment 5:

This point should be stated more cautiously.The site is influenced by local urban sources such as traffic, combustion, construction, and dust. The authors should briefly discuss how these emissions may affect NPF interpretation.

Response 5：

We thank the referee for this important comment. We agree that local urban emissions may influence both the measured ultrafine-particle population and the interpretation of NPF at the TU site. We have therefore expanded the site description and the discussion of urban-source influences. Traffic and combustion emissions may provide gaseous precursors and directly emitted ultrafine particles, whereas construction activities and resuspended dust may increase the pre-existing aerosol population and particle sink, thereby affecting the survival and growth of newly formed particles.

To reduce confusion between atmospheric NPF and short-lived primary-emission plumes, the revised classification does not rely solely on an increase in small-particle number concentration. An NPF day requires the appearance of a distinct new particle mode at small diameters followed by identifiable growth toward larger sizes. Short-lived particle-number spikes without subsequent systematic growth were not classified as NPF. The size-segregated diurnal analysis further showed that the morning increase in N_{3-25} on NPF days was followed by an enhancement in N_{25-100}, supporting the interpretation of particle formation and subsequent growth. In contrast, evening enhancements in Aitken-mode particles without a preceding nucleation-mode increase may have been influenced by local urban emissions and are now interpreted cautiously.

We also examined SO_2, NO_2, and O_3 under different wind directions on NPF and non-NPF days (Figs. 8 and 9). The results showed differences in gaseous pollutants and transport conditions between day types, but no single wind sector or short-lived gaseous-pollutant enhancement consistently explained all identified NPF events.

Because BC measurements were unavailable, we additionally examined the diurnal variations in $PM_{2.5}$ and PM_{10} for the revised day categories during both observation periods (Fig. R1). During the principal particle-formation period, the increase in nucleation-mode particle number concentration on NPF days was not accompanied by corresponding daytime spikes in $PM_{2.5}$ or PM_{10}. Daytime $PM_{2.5}$ concentrations were not higher on NPF days than on Non-Event days, whereas PM_{10} concentrations were broadly comparable between the two categories. These results suggest that the identified events were not simply manifestations of broader fine-particle pollution or dust episodes.

Nevertheless, $PM_{2.5}$ and PM_{10} are mass-based measurements dominated by larger particles and cannot substitute for BC as direct tracers of traffic-related ultrafine-particle emissions. Moreover, measurements were available at only one fixed site. We therefore cannot completely separate regional-scale NPF from all local primary ultrafine-particle influences or determine the spatial extent of individual events. We have explicitly acknowledged this limitation and avoid describing the identified events as definitively regional. Instead, they are interpreted as atmospheric NPF events observed at an urban site, while recognizing that local emissions may affect precursor availability, particle sinks, and parts of the measured ultrafine-particle population.

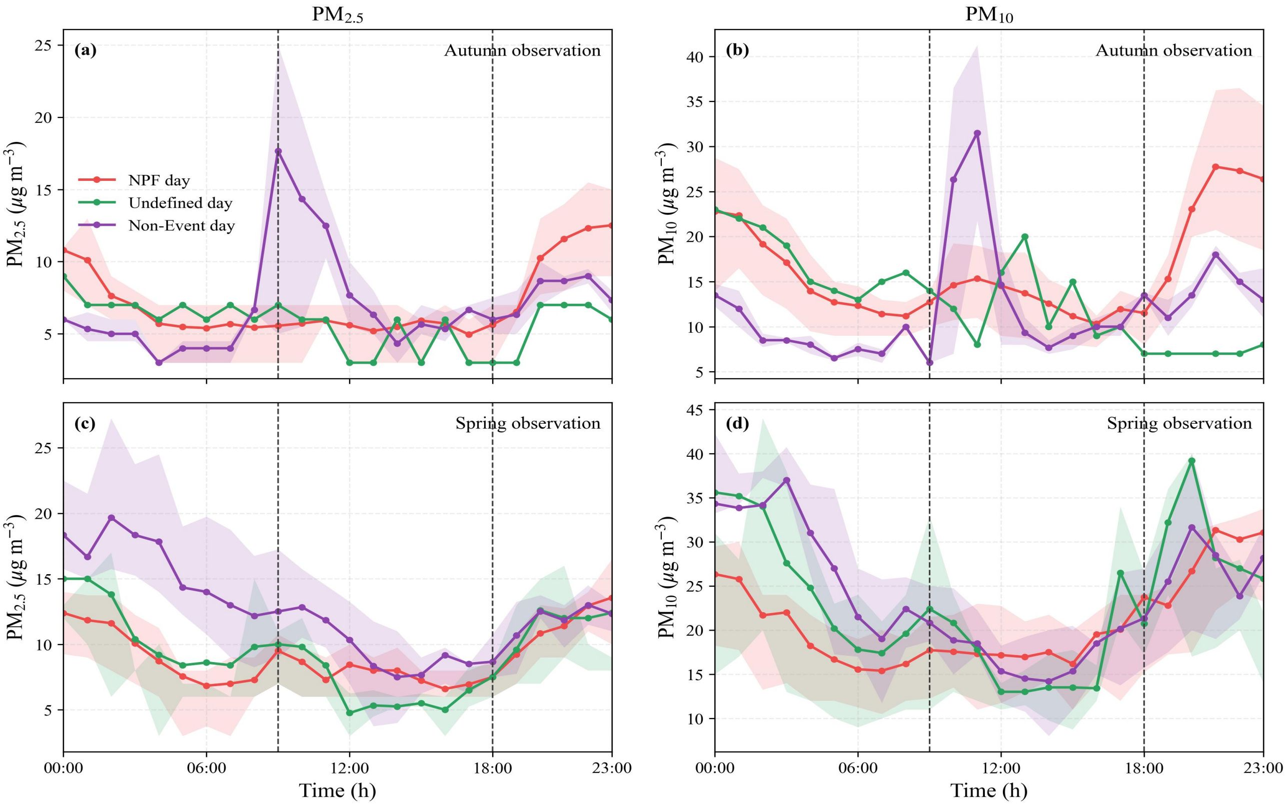

Figure R1. Diurnal variations in $PM_{2.5}$ and PM_{10} concentrations for NPF, Undefined, and Non-Event days during the autumn and spring observation periods. Solid lines represent hourly mean concentrations, and the shaded areas indicate the interquartile ranges. The vertical dashed lines indicate 09:00 and 18:00 local time. $PM_{2.5}$ and PM_{10} are used as supporting indicators of broader particulate-matter pollution and dust influences rather than as direct tracers of traffic-related ultrafine-particle emissions.

Comment 6:

I strongly recommend the authors should consider citing the study "Comprehensive spatiotemporal analysis of long-term mobile monitoring for traffic-related particles in a complex urban environment" in the Introduction or site-description discussion, as it provides relevant context on traffic-related particle variability in complex urban environments.

Response 6:

We thank the referee for recommending this relevant study. We have cited Yeganeh et al. (2026) in the site-description and urban-emission discussion. The added text highlights that traffic-related $PM_{2.5}$ and BC can exhibit pronounced spatial and temporal heterogeneity within complex urban environments and that fixed-site observations may not fully capture localized emission hotspots. This reference provides useful context for interpreting the TU measurements and supports our acknowledgment that a single fixed site cannot completely characterize the spatial variability of urban traffic-related particles.

Table S1. Day-by-day revised classification, NPF timing, particle number characteristics, and candidate particle growth rates during the two observation periods. Mean N_{3-25} and N_{25-100} concentrations were calculated over 09:00–18:00 local time. Candidate GR_{3-7} and GR_{7-20} values were evaluated for every observation day by linear regression of automatically identified continuous modal trajectories. No R^2 threshold was applied. "NA" indicates that insufficient data or no sufficiently long and continuous trajectory was available.

Date	Revised classification	Original growth subgroup	NPF window	Mean N_{3-25} (# cm^{-3})	Mean N_{25-100} (# cm^{-3})	GR_{3-7} window	GR_{3-7} (nm h^{-1})	GR_{7-20} window	GR_{7-20} (nm h^{-1})
Oct 9, 2024	NPF day	Class II	8:40–14:30	16954	4977	08:42–09:12	4.26	09:17–14:27	1.62
Oct 10, 2024	NPF day	Class II	9:00–15:00	10803	4047	NA	NA	09:22–14:57	1.94
Oct 16, 2024	NPF day	Class I	9:00–21:00	19292	8532	09:02–09:32	3.90	09:37–17:57	0.93
Oct 17, 2024	NPF day	Class II	9:00–14:00	16605	5433	NA	NA	09:07–13:57	2.19
Oct 18, 2024	NPF day	Class II	8:40–14:30	16091	5005	08:42–09:27	3.47	09:32–14:27	1.35
Oct 19, 2024	NPF day	Class II	9:00–15:00	6346	3912	09:02–09:37	1.80	09:42–14:57	2.35
Oct 20, 2024	NPF day	Class II	9:00–18:00	21295	6244	09:02–13:07	0.17	09:42–17:52	1.30
Oct 22, 2024	NPF day	Class I	9:00–22:00	20350	6818	09:02–16:37	-0.02	09:37–17:57	-0.42
Oct 23, 2024	NPF day	Class II	9:00–15:00	12206	4174	NA	NA	09:02–14:57	0.93
Oct 24, 2024	NPF day	Class I	9:00–23:00	11971	4732	09:02–09:32	5.30	09:37–17:57	0.53
Oct 25, 2024	NPF day	Class I	9:00–21:00	11913	4686	09:02–09:47	3.60	09:52–17:57	1.21
Oct 26, 2024	NPF day	Class I	9:30–23:00	12083	3157	09:32–13:52	0.08	10:07–17:57	1.06
Oct 27, 2024	NPF day	Class I	9:30–22:00	15552	6391	NA	NA	09:47–17:57	1.28
Oct 28, 2024	NPF day	Class I	9:00–24:00	16668	5924	NA	NA	09:22–17:57	1.10
Oct 29, 2024	NPF day	Class I	9:30–24:00	10131	5355	NA	NA	09:47–17:57	1.43
Oct 30, 2024	NPF day	Class I	9:30–24:00	8331	4331	NA	NA	09:52–17:57	1.12
Oct 31, 2024	NPF day	Class I	9:30–21:00	9420	6128	NA	NA	10:02–17:57	0.78
Nov 1, 2024	NPF day	Class I	9:30–24:00	18403	6892	NA	NA	10:02–17:57	0.85
Nov 2, 2024	NPF day	Class I	9:00–24:00	19211	7233	09:02–09:32	5.17	09:37–17:57	1.16

Date	Revised classification	Original growth subgroup	NPF window	Mean $N_{3–25}$ (# cm^{-3})	Mean $N_{25–100}$ (# cm^{-3})	$GR_{3–7}$ window	$GR_{3–7}$ (nm h^{-1})	$GR_{7–20}$ window	$GR_{7–20}$ (nm h^{-1})
Nov 3, 2024	NPF day	Class I	9:00–21:00	14440	6669	09:02–09:52	3.13	09:57–17:57	1.31
Nov 4, 2024	NPF day	Class II	12:00–16:00	4937	3492	NA	NA	12:02–15:57	3.34
Nov 7, 2024	NPF day	Class I	9:00–24:00	24496	8216	NA	NA	09:27–17:57	0.49
Nov 8, 2024	NPF day	Class I	9:30–24:00	16717	8280	NA	NA	09:52–17:57	0.72
Nov 9, 2024	NPF day	Class I	9:30–24:00	14049	6956	NA	NA	09:42–17:57	1.08
Nov 10, 2024	NPF day	Class I	9:30–24:00	10546	5078	NA	NA	10:02–17:57	1.34
Mar 25, 2025	NPF day	Class I	9:00–21:00	13321	3237	NA	NA	09:25–18:00	1.05
Mar 26, 2025	NPF day	Class I	9:00–21:00	8415	3265	09:00–09:35	3.36	09:40–18:00	1.17
Mar 27, 2025	NPF day	Class II	9:00–17:00	15776	3581	NA	NA	09:20–17:00	0.60
Mar 28, 2025	NPF day	Class II	9:00–14:00	12317	2713	NA	NA	09:20–13:40	2.22
Mar 30, 2025	NPF day	Class II	9:00–11:00	3715	561	09:00–09:35	4.33	09:40–10:55	4.73
Apr 2, 2025	NPF day	Class II	8:30–12:30	7511	1182	08:30–09:35	1.67	09:40–12:30	1.49
Apr 6, 2025	NPF day	Class II	8:30–13:00	13406	1586	NA	NA	08:30–12:55	0.98
Apr 7, 2025	NPF day	Class II	8:30–12:30	8616	2079	08:30–09:00	5.78	09:05–12:25	2.16
Apr 8, 2025	NPF day	Class II	8:30–16:30	9734	1750	08:30–09:10	3.92	09:15–16:25	0.95
Apr 9, 2025	NPF day	Class II	9:00–16:00	6494	3110	09:00–09:35	3.48	09:40–15:55	1.60
Apr 12, 2025	NPF day	Undefined	9:00–11:00	4131	2176	NA	NA	09:20–10:55	8.44
Apr 13, 2025	NPF day	Class II	9:00–16:00	9928	2010	09:00–09:40	3.51	09:45–15:55	1.22
Apr 16, 2025	NPF day	Class II	8:30–16:00	11387	5571	NA	NA	09:00–15:55	1.28
Apr 17, 2025	NPF day	Class I	8:00–18:00	16775	6852	NA	NA	08:30–17:55	1.03
Apr 18, 2025	NPF day	Undefined	11:00–14:00	5239	1392	NA	NA	11:25–13:55	1.59
Apr 19, 2025	NPF day	Class II	8:30–18:00	10978	3950	NA	NA	08:50–17:55	1.15

Date	Revised classification	Original growth subgroup	NPF window	Mean $N_{3–25}$ (# cm^{-3})	Mean $N_{25–100}$ (# cm^{-3})	$GR_{3–7}$ window	$GR_{3–7}$ (nm h^{-1})	$GR_{7–20}$ window	$GR_{7–20}$ (nm h^{-1})
Apr 21, 2025	NPF day	Class I	8:00–21:00	15983	4139	08:00–08:30	2.95	08:35–17:55	0.93
Apr 22, 2025	NPF day	Class II	9:00–16:00	9488	1375	NA	NA	09:15–15:55	0.46
Oct 15, 2024	Undefined	Undefined	NA	2042	1142	07:17–12:57	-0.14	07:02–17:57	0.44
Mar 29, 2025	Undefined	Undefined	NA	2946	644	13:35–14:25	0.67	07:00–17:55	-0.28
Apr 10, 2025	Undefined	Undefined	NA	3888	819	NA	NA	07:00–17:55	-0.05
Apr 11, 2025	Undefined	Undefined	NA	5214	989	NA	NA	07:00–17:45	-0.02
Apr 14, 2025	Undefined	Undefined	NA	2597	1219	NA	NA	07:05–17:55	0.60
Apr 20, 2025	Undefined	Undefined	NA	4855	873	NA	NA	07:20–17:55	0.40
Oct 21, 2024	Non-Event	Non-Event	NA	2011	1117	12:32–13:42	-0.72	07:02–17:57	0.39
Nov 5, 2024	Non-Event	Non-Event	NA	1034	2292	07:12–17:57	-0.25	07:02–17:17	0.80
Nov 6, 2024	Non-Event	Non-Event	NA	1085	2751	NA	NA	07:02–17:57	-0.35
Mar 31, 2025	Non-Event	Non-Event	NA	517	366	14:35–17:00	0.07	07:00–17:15	-0.88
Apr 1, 2025	Non-Event	Non-Event	NA	170	410	13:50–14:25	0.52	14:30–18:00	0.49
Apr 3, 2025	Non-Event	Non-Event	NA	688	401	07:35–10:55	-0.19	07:00–18:00	-0.15
Apr 4, 2025	Non-Event	Non-Event	NA	245	443	NA	NA	07:20–18:00	-0.01
Apr 5, 2025	Non-Event	Non-Event	NA	254	585	NA	NA	07:00–17:55	0.16
Apr 15, 2025	Non-Event	Non-Event	NA	846	1023	NA	NA	07:00–17:35	-0.37

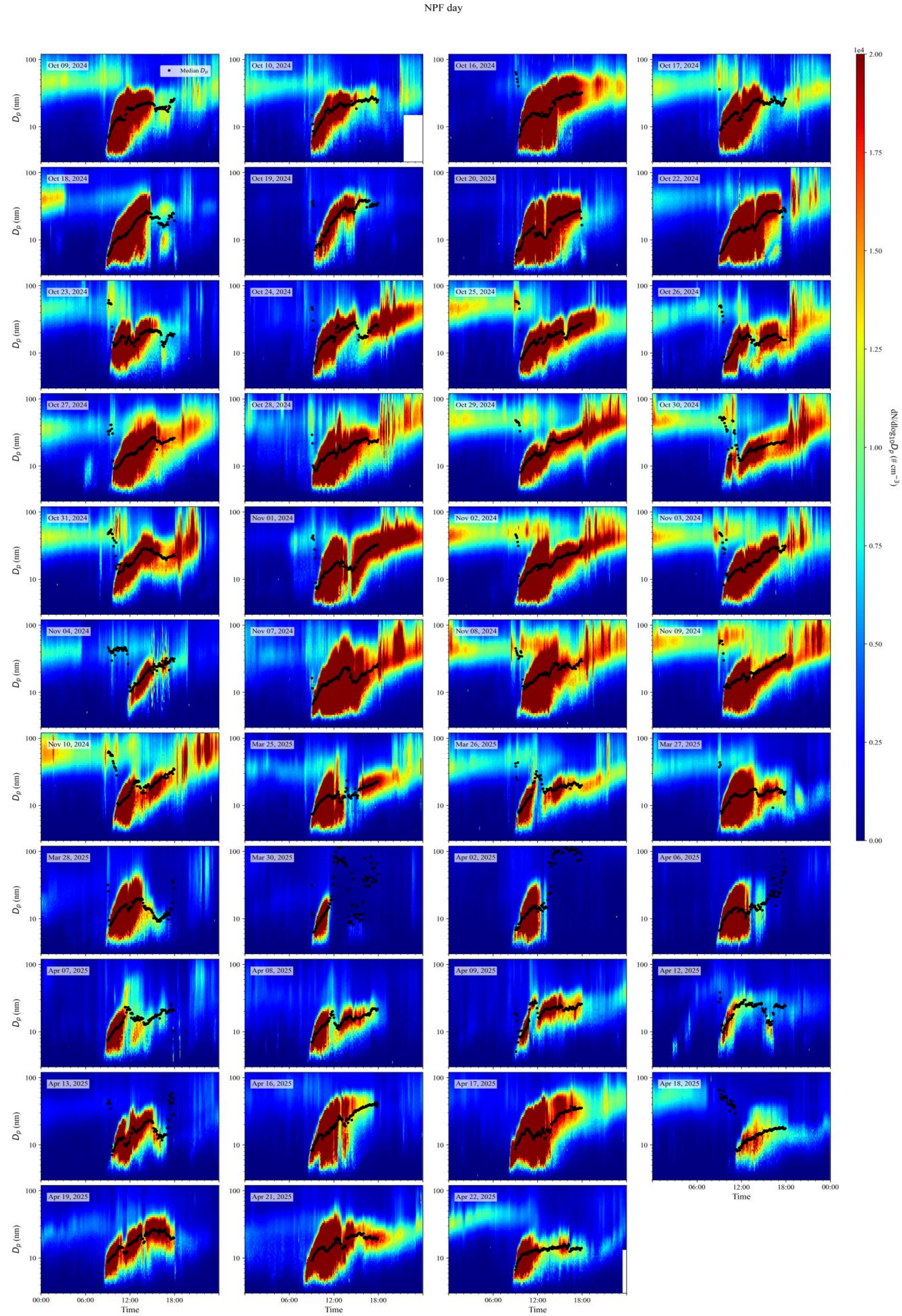

Figure S1: PNSDs for all NPF days. Each panel represents one day. The black dots indicate the median particle diameter.

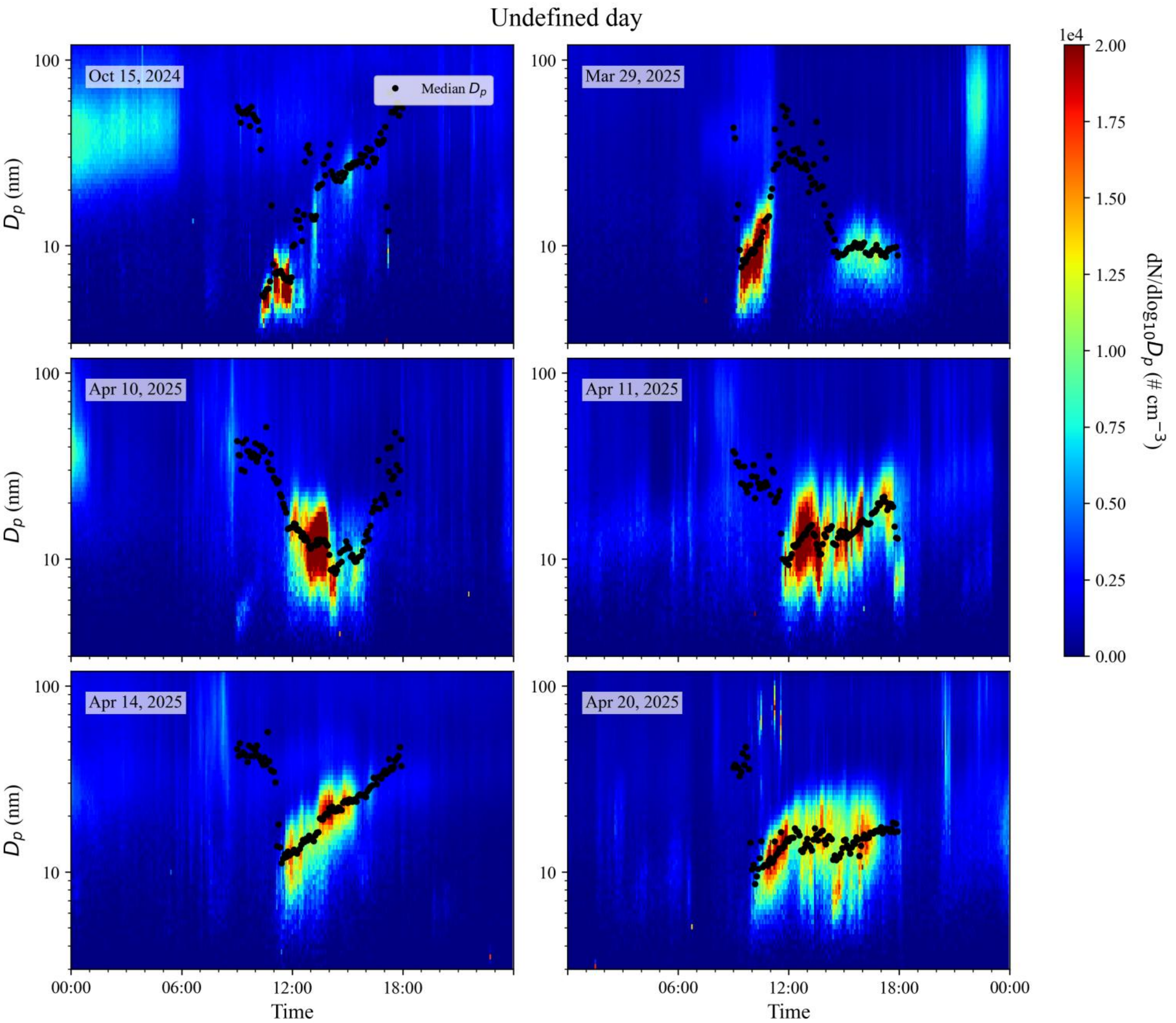

Figure S2: PNSDs for all Undefined days. Each panel represents one day. The black dots indicate the median particle diameter.

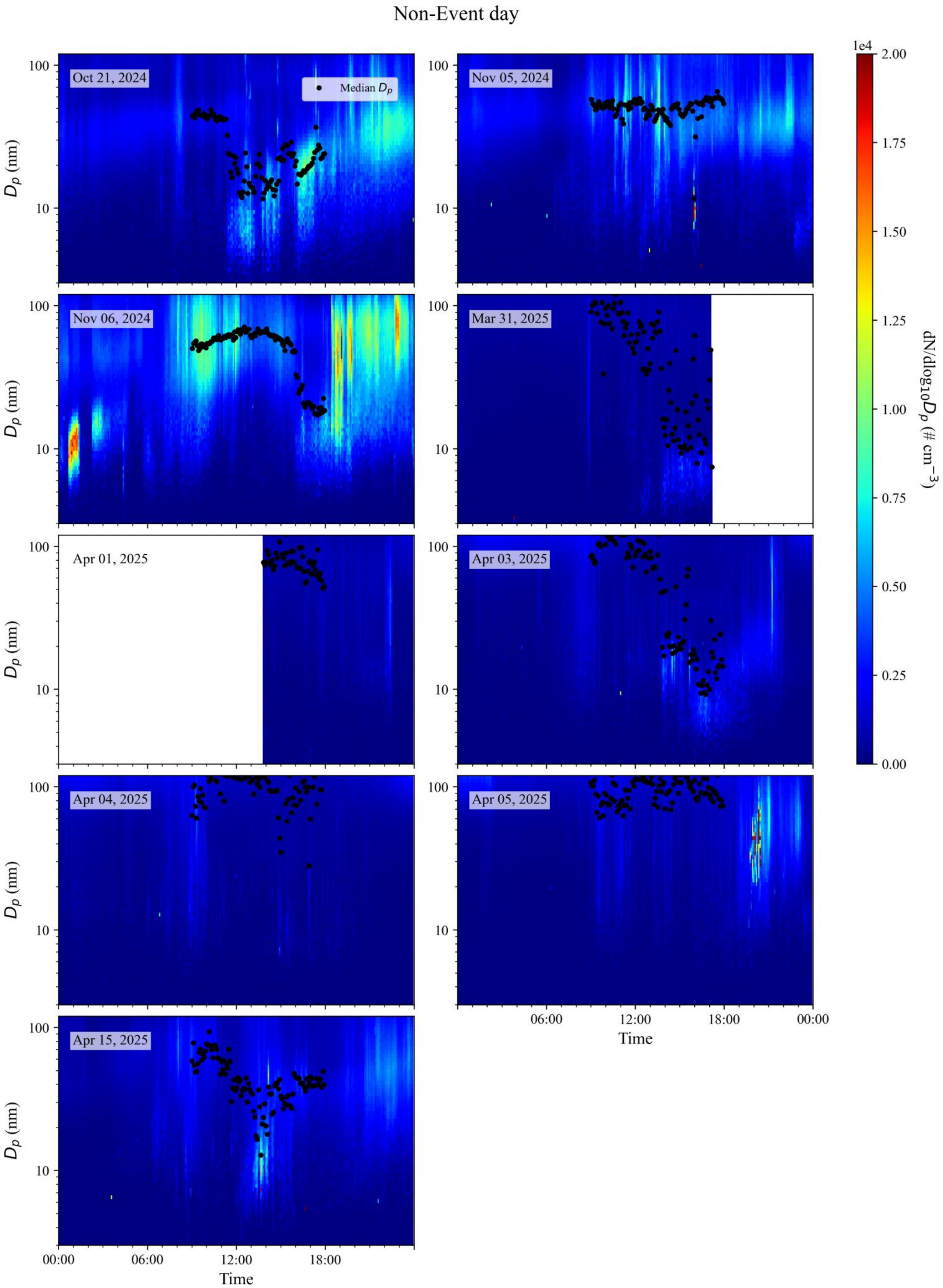

Figure S3: PNSDs for all Non-Event days. Each panel represents one day. The black dots indicate the median particle diameter.

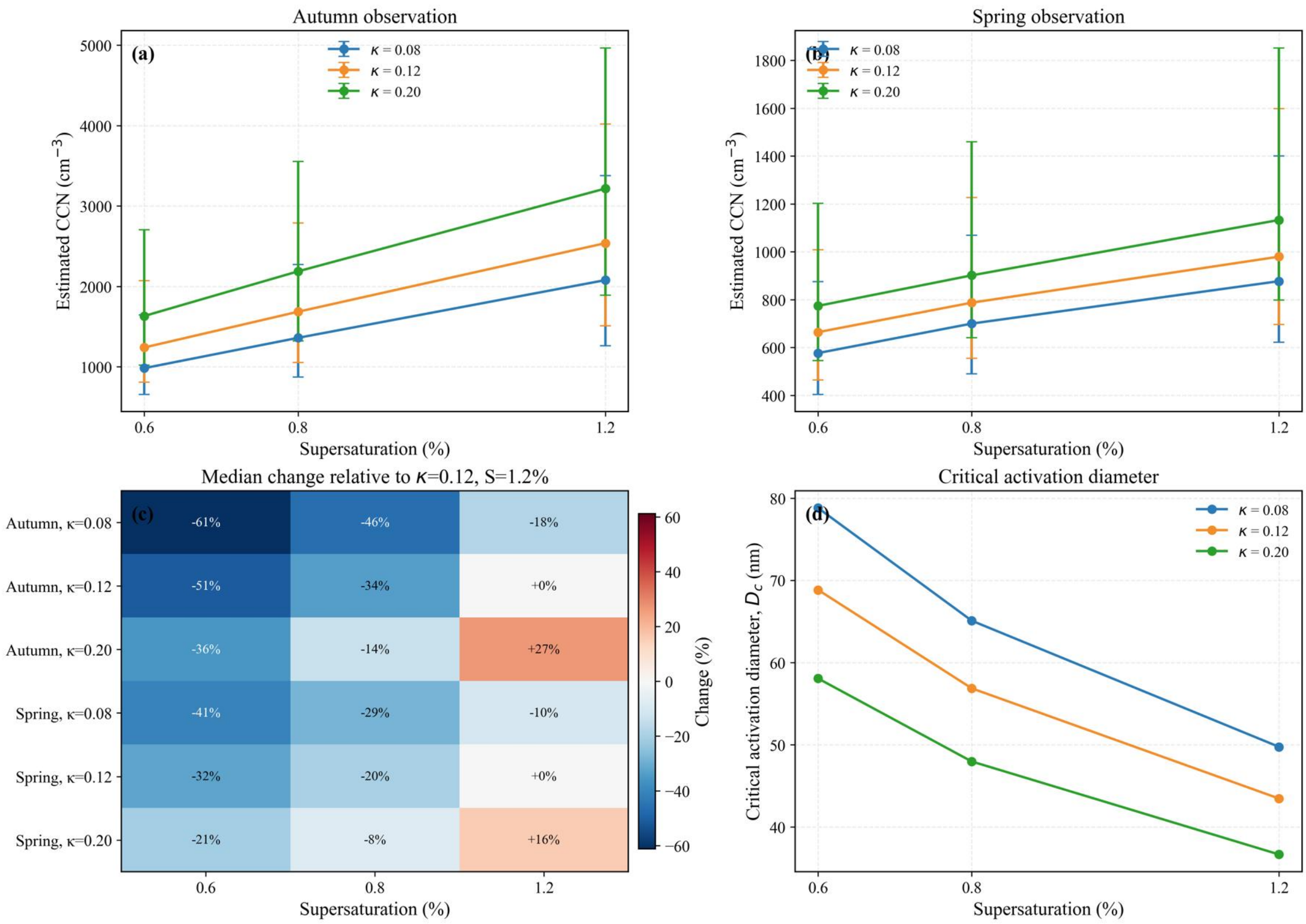

Figure S7. Sensitivity of estimated CCN concentrations and critical activation diameter to the assumed particle hygroscopicity parameter (κ) and supersaturation (S). Panels (a) and (b) show the median estimated CCN concentrations, with error bars representing the interquartile range, under different κ and S assumptions during the autumn and spring observation periods, respectively. Panel (c) shows the percentage change in median CCN relative to the baseline assumptions of κ = 0.12 and S = 1.2 %. Panel (d) shows the corresponding critical activation diameters.